

1 **Title: Simultaneous disintegration of outlet glaciers in Porpoise Bay (Wilkes Land),**
2 **East Antarctica, driven by sea-ice break-up.**

3 **Authors:** B.W.J. Miles^{1*}, C. R. Stokes¹, S.S.R. Jamieson¹

4 **Affiliation:** ¹Department of Geography, Durham University, Science Site, South Road, Durham, DH1 3LE,

5 UK

6 **Correspondence to:* a.w.j.miles@durham.ac.uk

7
8 **Abstract:** The floating ice shelves and glacier tongues which fringe the Antarctic
9 continent are important because they help buttress ice flow from the ice sheet interior.
10 Dynamic feedbacks associated with glacier calving have the potential to reduce
11 buttressing and subsequently increase ice flow into the ocean. However, there are few
12 high temporal resolution studies on glacier calving, especially in East Antarctica. Here
13 we use ENVISAT ASAR wide swath mode imagery to investigate monthly glacier
14 terminus change across six marine-terminating outlet glaciers in Porpoise Bay (-76°S,
15 128°E), Wilkes Land (East Antarctica), between November 2002 and March 2012. This
16 reveals a large near-simultaneous calving event in January 2007, resulting in a total of
17 ~2,900 km² of ice being removed from glacier tongues. We also observe the start of a
18 similar large near-simultaneous calving event in March 2016. Our observations suggest
19 that both of these large calving events are driven by the break-up of the multi-year sea-
20 ice which usually occupies Porpoise Bay. However, these break-up events appear to
21 have been driven by contrasting mechanisms. We link the 2007 sea-ice break-up to
22 atmospheric circulation anomalies in December 2005 weakening the multi-year sea-ice
23 through a combination of surface melt and a change in wind direction prior to its
24 eventual break-up in January 2007. In contrast, the 2016 break-up event is linked to the
25 terminus of Holmes (West) Glacier pushing the multi-year sea-ice further into the open
26 ocean, making the sea-ice more vulnerable to break-up. In the context of predicted
27 future warming and the sensitivity of sea-ice to changes in climate, our results highlight
28 the importance of interactions between landfast sea-ice and glacier tongue stability in
29 East Antarctica.

30

31 **1. Introduction**

32 Iceberg calving is an important process that accounts for around 50% of total mass loss to the
33 ocean in Antarctica (Depoorter et al., 2013; Rignot et al., 2013). Moreover, dynamic
34 feedbacks associated with retreat and/or thinning of buttressing ice shelves or floating glacier
35 tongues can result in an increased discharge of ice into the ocean (Rott et al., 2002; Rignot et
36 al., 2004; Wuite et al., 2015; Fürst et al., 2016). At present, calving dynamics are only
37 partially understood (Benn et al., 2007; Chapuis and Tetzlaff, 2014) and models struggle to
38 replicate observed calving rates (van der Veen, 2002; Astrom et al., 2014). Therefore,
39 improving our understanding of the mechanisms driving glacier calving and how glacier
40 calving cycles have responded to recent changes in the ocean-climate system is important in
41 the context of future ice sheet mass balance and sea level.

42 Calving is a two-stage process that requires both the initial ice fracture and the subsequent
43 transport of the detached iceberg away from the calving front (Bassis and Jacobs, 2013). In
44 Antarctica, major calving events can be broadly classified into two categories: the discrete
45 detachment of large tabular icebergs (e.g. Mertz glacier tongue: Massom et al., 2015) or the
46 spatially extensive disintegration of floating glacier tongues or ice shelves into numerous
47 smaller icebergs (e.g. Larsen A & B ice shelves (Rott et al., 1996; Scambos et al., 2009).
48 Observations of decadal-scale changes in glacier terminus position in both the Antarctic
49 Peninsula and East Antarctica have suggested that despite some degree of stochasticity,
50 iceberg calving and glacier advance/retreat is likely driven by external climatic forcing (Cook
51 et al., 2005; Miles et al., 2013). However, despite some well-documented ice shelf collapses
52 (Scambos et al., 2003; Banwell et al., 2013) and major individual calving events (Masson et
53 al., 2015) there is a paucity of data on the nature and timing of calving from glaciers in
54 Antarctica (e.g. compared to Greenland: Moon and Joughin, 2008; Carr et al., 2013), and
55 particularly in East Antarctica.

56 Following recent work that highlighted the potential vulnerability of the East Antarctic Ice
57 Sheet in Wilkes Land to ocean-climate forcing and marine ice sheet instability (Greenbaum et
58 al., 2015; Aitken et al., 2016; Miles et al., 2013; 2016), we analyse the recent calving activity
59 of six outlet glaciers in the Porpoise Bay region using monthly satellite imagery between
60 November 2002 and March 2012. In addition, we also observe the start of a large calving
61 event in 2016. We then turn our attention to investigating the drivers behind the observed
62 calving dynamics.

63 **2. Study area**

64 Porpoise Bay (-76°S, 128°E) is situated in Wilkes Land, East Antarctica, approximately 300
65 km east of Moscow University Ice Shelf and 550 km east of Totten glacier (Fig. 1). This area
66 was selected for study because it occupies a central position in Wilkes Land, which is thought
67 to have experienced mass loss over the past decade (King et al., 2012; Sasgen et al., 2013;
68 McMillan et al., 2014), and which is the only region of East Antarctica where the majority of
69 marine-terminating outlet glaciers have experienced recent (2000-2012) retreat (Miles et al.,
70 2016). This is particularly concerning because Wilkes Land overlies the Aurora subglacial
71 basin and, due its reverse bed slope and deep troughs (Young et al., 2011), it may have been
72 susceptible to unstable grounding line retreat in the past (Cook et al., 2014), and could make
73 significant contributions to global sea level in the future (DeConto and Pollard, 2016).
74 However, despite some analysis on glacier terminus position on a decadal timescales
75 (Frezzotti and Polizzi, 2002; Miles et al., 2013; 2016), there has yet to be any investigation of
76 inter-annual and sub-annual changes in terminus position and calving activity in the region.

77 Porpoise Bay is 150 km wide and is typically filled with land-fast multi-year sea-ice (Fraser
78 et al., 2012). In total, six glaciers were analysed, with glacier velocities (from Rignot et al.,
79 2011) ranging from ~440 m yr⁻¹ (Sandford Glacier) to ~2000 m yr⁻¹ (Frost Glacier). Recent
80 studies have suggested that the largest (by width) glacier feeding into the bay - Holmes
81 Glacier - has been thinning over the past decade (Pritchard et al., 2009; McMillan et al.,
82 2014).

83 **3. Methods**

84 **3.1 Satellite imagery and terminus position change**

85 Glacier terminus positions were mapped at approximately monthly intervals between
86 November 2002 and March 2012, using Envisat Advanced Synthetic Aperture Radar (ASAR)
87 Wide Swath Mode (WSM) imagery across six glaciers, which were identified from the
88 Rignot et al. (2011b) ice velocity dataset (Fig.1). Additional sub-monthly imagery between
89 December 2006 and April 2007 were used to gain a higher temporal resolution following the
90 identification of a major calving event around that time. During the preparation for this
91 manuscript we also observed the start of another large calving event, which we observed with
92 Sentinel-1 imagery (Table 1).

93 Approximately 65% of all glacier frontal measurements were made using an automated
94 mapping method. This was achieved by automatically classifying glacier tongues and sea-ice
95 into polygons based on their pixel values, with the boundary between the two taken as the
96 terminus position. The threshold between glacial ice and sea-ice was calculated automatically
97 based on the image pixel statistics, whereby sea-ice appears much darker than the glacial ice.
98 In images where the automated method was unsuccessful, terminus position was mapped
99 manually. The majority of these manual measurements were undertaken in the austral
100 summer (December – February) when automated classification was especially problematic
101 due to the high variability in backscatter on glacier tongues as a result of surface melt.
102 Following the mapping of the glacier termini, length changes were calculated using the box
103 method (Moon and Joughin, 2008). This method calculates the glacier area change between
104 each time step divided by the width of the glacier, to give an estimation of glacier length
105 change. The width of glacier was obtained by a reference box which approximately delineates
106 the sides of the glacier.

107 Given the nature of the heavily fractured glacier fronts and the moderate resolution of Envisat
108 ASAR WSM imagery (80 m) it was sometimes difficult to establish if individual or blocks of
109 icebergs were attached to the glacier tongue. As a result, there are errors in precisely
110 determining terminus change on a monthly time-scale ($\sim\pm 500$ m). However, because our
111 focus is on major calving events, absolute terminus position is less important than the
112 identification of major episodes of calving activity. Indeed, because estimations of terminus
113 position were made at approximately monthly intervals, calving events were easily
114 distinguished because the following month's estimation of terminus position would clearly
115 show the glacier terminus in a retreated position. In addition, each image was also checked
116 visually to make sure no small calving events were missed (i.e. as indicated by the presence
117 of icebergs proximal to the glacier tongue).

118 **3.2 Sea-ice**

119 Sea-ice concentrations in Porpoise Bay were calculated using mean monthly Bootstrap sea-
120 ice concentrations derived from the Nimbus-7 satellite and the Defence Meteorological
121 Satellite Program (DMSP) satellites which offers near complete coverage between October
122 1978 and December 2014 (Comiso, 2014; <http://dx.doi.org/10.5067/J6JQLS9EJ5HU>). To
123 extend the sea-ice record, we also use mean monthly Nimbus-5 Electrically Scanning
124 Microwave Radiometer (ESMR) derived sea-ice concentrations (Parkinson et al., 2004;

125 https://nsidc.org/data/docs/daac/nsidc0009_esmr_seaice.gd.html), which offer coverage
126 between December 1972 and March 1977. However, from March to May 1973, August 1973,
127 April 1974 and June to August 1975, mean monthly sea-ice concentrations were not
128 available. Sea-ice concentrations were extracted from 18 grid cells, covering 11,250 km² that
129 extended across Porpoise Bay, but not into the extended area beyond the limits of the bay
130 (Fig. 1). Grid cells which were considered likely to be filled with glacial ice were excluded.
131 Pack ice concentrations were also extracted from a 250 x 150 km polygon adjacent to
132 Porpoise Bay. The dataset has a spatial resolution of 25 km and monthly sea-ice
133 concentration anomalies were calculated from the 1972-2016 monthly mean.

134 Daily sea-ice concentrations derived from the Artist Sea-Ice (ASI) algorithm from Advanced
135 Microwave Scanning Radiometer - EOS (AMSR-E) data (Spren et al., 2008) were used to
136 calculate daily sea-ice concentration anomalies during the January 2007 sea-ice break-up
137 (<http://icdc.zmaw.de/1/daten/cryosphere/seaiceconcentration-asi-amsre.html>). This dataset
138 was used because it provides a higher spatial resolution (6.25 km) compared to those
139 available using Bootstrap derived concentrations (25 km). This is important because it
140 provides a more accurate representation of when sea-ice break-up was initiated and, due to its
141 much higher spatial resolution, it provides data from much closer to the glacier termini (see
142 Fig.1).

143 **3.3 RACMO**

144 We used the Regional Atmospheric Climate Model (RACMO) V2.3 (van Wessem et al., 2014)
145 to simulate daily surface melt fluxes in the study area between 1979 and 2015 at a 27 km
146 spatial resolution. The melt values were extracted from floating glacier tongues in Porpoise
147 Bay because the model masks out sea-ice, equating to seven grid points. The absolute surface
148 melt values are likely to be different on glacial ice, compared to the sea-ice, but the relative
149 magnitude of melt is likely to be similar temporally.

150 **3.4 ERA-interim**

151 In the absence of weather stations in the vicinity of Porpoise Bay we use the 0.25° ERA-
152 interim reanalysis dataset ([http://apps.ecmwf.int/datasets/data/interim-full-](http://apps.ecmwf.int/datasets/data/interim-full-modala/levtype=sfc/)
153 [modala/levtype=sfc/](http://apps.ecmwf.int/datasets/data/interim-full-modala/levtype=sfc/)) to calculate mean monthly wind field and sea surface temperature (SST)
154 anomalies, with respect to the 1979-2015 monthly mean. Wind field anomalies were
155 calculated by using the mean monthly 10 m zonal (U) and meridional (V) wind components.

156 We also used the daily 10 m zonal (U) and meridional (V) components to simulate wind field
157 vectors in Porpoise Bay on January 11th 2007 and March 19th 2016 which are the estimated
158 dates of sea-ice break-up.

159 **4. Results**

160 **4.1 Terminus position change**

161 Analysis of glacier terminus position change of six glaciers in Porpoise Bay between
162 November 2002 and March 2012 reveals three broad patterns of glacier change (Fig. 2). The
163 first pattern is shown by Holmes (West) glacier, which advances a total of ~13 km throughout
164 the observation period, with no evidence of any major iceberg calving that resulted in
165 substantial retreat of the terminus beyond the measurement error (+/- 500 m). The second is
166 shown by Sandford Glacier tongue, which advanced ~1.5 km into the ocean between
167 November 2002 and April 2006, before its floating tongue broke away in May 2006. A further
168 smaller calving event was observed in January 2009. Overall, by the end of the study period,
169 its terminus had retreated around 1 km from its position in November 2002. The third pattern is
170 shown by Frost Glacier, Glacier 1, Glacier 2 and Holmes (East) glaciers, which all advanced
171 between November 2002 and January 2007, albeit with a small calving event in Frost glacier in
172 May 2006. However, between January and April 2007, Frost Glacier, Glacier 1, Glacier 2 and
173 Holmes (East) glaciers all underwent a large near-simultaneous calving event. This led to
174 1,300 km² of ice being removed from glaciers in Porpoise Bay, although we also note the
175 disintegration of a major tongue from an unnamed glacier further west, which contributed a
176 further 1,600 km². Thus, in a little over three months, a total of 2,900 km² of ice was removed
177 from glacier tongues in the study area (Fig. 3). Following this calving event, the fronts of these
178 glaciers stabilised and began advancing at a steady rate until the end of the study period
179 (March, 2012) (Fig. 2), with the exception of Frost glacier which underwent a small calving
180 event in April 2010.

181 **4.2 Evolution of the 2007 calving event**

182 A series of eight sub-monthly images between December 11th 2006 and April 8th 2007 show
183 the evolution of the 2007 calving event (Fig. 4). Between December 11th 2006 and January 2nd
184 2007, the land-fast sea-ice edge retreats past Sandford glacier to the edge of Frost glacier and
185 there is some evidence of sea-ice fracturing in front of the terminus of Glacier 2 (Fig. 4b).
186 From January 2nd to January 9th a small section (~40 km²) of calved ice broke away from Frost

187 glacier, approximately in line with the retreat edge of land-fast sea-ice (Fig. 4c). By January
188 25th, significant fracturing in the land-fast sea-ice had developed, and detached icebergs from
189 Frost, Glacier 1, Glacier 2 and Holmes East glaciers begin to breakaway (Fig. 4d). This process
190 of rapid sea-ice breakup in the east section of the bay and the disintegration of sections of Frost
191 glacier, Glacier 1, Glacier 2 and Holmes East glaciers continues up to March 10th 2007 (Fig.
192 4g). In contrast, the west section of Porpoise Bay remains covered in sea-ice in front of
193 Holmes west glacier, which does not calve throughout this event. By April 8th, the calving
194 event had ended with a large number of calved icebergs now occupying the bay (Fig. 4h).

195 **4.3 2016 calving event**

196 During the preparation of this manuscript satellite observations of Porpoise Bay revealed that
197 another large near-simultaneous disintegration of glacier tongues in Porpoise Bay is currently
198 underway. This event was initiated on March 19th where the edge of the multi-year sea-ice
199 retreated to the Holmes West glacier terminus, removing multi-year sea-ice which was at
200 least 14 years old. By March 24th this had led to the rapid disintegration of an 800 km²
201 section of the Holmes West glacier tongue (Fig. 5). This was the first observed calving of
202 Holmes (West) glacier at any stage between November 2002 and March 2016. Throughout
203 March and April the break-up of sea-ice continued and by May 13th it had propagated to the
204 terminus of Frost Glacier, resulting in the disintegration of large section of its tongue (Fig. 6).
205 By 24th July sea-ice had been removed from all glacier termini in Porpoise Bay at some point
206 during the event, resulting in a total of ~2,200 km² ice being removed from glacier tongues
207 (Fig. 6).

208 **4.4. The link between sea-ice and calving in Porpoise Bay**

209 Analysis of mean monthly sea-ice concentration anomalies in Porpoise Bay between
210 November 2002 and June 2016 (Fig. 7) reveals a major negative sea-ice anomaly occurred
211 between January and June 2007, where monthly sea-ice concentrations were between 35%
212 and 40% below average. This is the only noticeable (>20%) negative ice anomaly in Porpoise
213 Bay and it coincides with the major January 2007 calving event (see Fig. 4). However,
214 despite satellite imagery showing the break-up of sea-ice prior to the 2016 calving event (Fig.
215 5 and 6), in a similar manner to that in 2007 (e.g. Fig. 4), no large negative anomaly is
216 present in the sea-ice concentration data. This is likely to reflect the production of a large
217 armada of icebergs following the disintegration of Holmes (West) Glacier (e.g. Fig. 6) ,
218 helping promote a rapid sea-ice reformation in the vicinity of Porpoise Bay. Furthermore, we

219 note that the smaller calving events of Sandford and Frost glaciers all take place after sea-ice
220 had retreated away from the glacier terminus (Fig. 8). Indeed, throughout the study period,
221 there is no evidence of any calving events taking place with sea-ice proximal to glacier
222 termini. This suggests that glaciers in Porpoise Bay are very unlikely to calve with sea-ice
223 present at their termini.

224 **4.5. Atmospheric circulation anomalies**

225 Atmospheric circulation anomalies in the months preceding the January 2007 and March
226 2016 sea-ice break-ups reveal contrasting conditions. In the austral summer which preceded
227 the January 2007 break-up there were strong positive SST anomalies and atmospheric
228 circulation anomalies throughout December 2005 (Fig. 9a). The circulation anomaly was
229 reflected in a strong easterly airflow offshore from Porpoise Bay. This is associated with a
230 band of cooler SSTs close to the coastline and the northward shift of the Antarctic Coastal
231 Current in response to the weakened westerlies (e.g. Langlais et al., 2015). A weakened zonal
232 flow combined with high sea surface temperatures (SST) in the south Pacific would allow the
233 advection of warmer maritime air into Porpoise Bay. Consistent with warmer air are
234 estimates of exceptionally high melt values in Porpoise Bay during December 2005 derived
235 from the RACMO2.3, which contrasts with the longer-term trend of cooling (Fig. 10).
236 However, the December 2005 anomaly was short-lived and, by January 2006, the wind field
237 conditions were close to average, although SST remained slightly higher than average (Fig.
238 9b).

239 In December 2006 and January 2007, which are the months immediately before and during
240 the break-up of sea-ice, atmosphere conditions were close to average, with very little
241 deviation from mean conditions in the wind field and a small negative SST anomaly (Fig.
242 9c). However, on January 11th 2007, which is the estimated date of sea-ice break-up from
243 AMSR-E data, we note that there were very high winds close to Porpoise Bay (Fig. 11a).

244 In contrast to the months preceding the January 2007 event, we find little deviations from
245 average conditions prior to the March 2016 break-up event. In the austral summer which
246 preceded the 2016 break-up (2014/15), there was little deviation from the average wind field
247 and only a small increase from average SSTs (Fig 9d). In December and January 2015/16,
248 there was evidence for a small increase in the strength of westerly winds, and cooler SSTs in
249 the South Pacific (Fig. 9e). However, in February and March 2016 there was no change from
250 the average wind field and slightly cooler SSTs (Fig. 9f). We note, however, that there was a

251 low pressure system passing across Porpoise Bay on March 19th 2016, the estimated date of
252 break-up initiation (Fig. 11b).

253 **4.6 Holmes (West) Glacier calving cycle**

254 Through mapping the terminus position in all available satellite imagery (Table 1) dating
255 back to 1963, we are able to reconstruct large calving events on the largest glacier in Porpoise
256 bay, Holmes (West) (Fig. 12). On the basis that a large calving event is likely during the
257 largest sea-ice break-up events, we estimate the date of calving based on sea-ice
258 concentrations in Porpoise Bay when satellite imagery is not available. Our estimates suggest
259 that Holmes (West) Glacier calves at approximately the same position in each calving cycle,
260 including the most recent calving event in March 2016.

261 **5. Discussion**

262 **5.1 Sea-ice break-up and the disintegration of glacier tongues in Porpoise Bay**

263 We report a major, near-synchronous calving event in January 2007 and a similar event that
264 was initiated in 2016 and resulted in $\sim 2,900 \text{ km}^2$ and $2,200 \text{ km}^2$ of ice, respectively, being
265 removed from glacier tongues in the Porpoise Bay region of East Antarctica. This is
266 comparable to some of the largest disintegration events ever observed in Antarctica (e.g.
267 Larsen A in 1995, $4,200 \text{ km}^2$ and Larsen B in 2002, $3,250 \text{ km}^2$); and is the largest event to have
268 been observed in East Antarctica. However, this event differs from those observed on the ice
269 shelves of the Antarctic Peninsula, in that it may be more closely linked to a cycle of glacier
270 advance and retreat, as opposed to a catastrophic collapse that may be unprecedented.

271 Given the correspondence between the sea-ice and glacier terminus changes, we suggest that
272 these disintegration events were driven by the break-up of the multi-year land-fast sea-ice
273 which usually occupies Porpoise Bay and the subsequent loss of buttressing of the glacier
274 termini. A somewhat similar mechanism has been widely documented in Greenland, where the
275 dynamics of sea-ice melange in proglacial fjords has been linked to inter-annual variations in
276 glacier terminus position (Amundson et al., 2010; Carr et al., 2013; Todd and Christoffersen,
277 2014; Cassotto et al., 2015). Additionally, the mechanical coupling between thick multi-year
278 landfast sea ice and glacier tongues may have acted to stabilize and delay the calving of the
279 Mertz glacier tongue (Massom et al., 2010) and Brunt/Stancomb-Wills Ice Shelf system
280 (Khazendar et al., 2009). However, this is the first observational evidence directly linking
281 multi-year landfast sea-ice break-up to the large scale and rapid disintegration of glacier

282 tongues. This is important because landfast sea-ice is highly sensitive to climate (Heil, 2006;
283 Mahoney et al., 2007) and, if future changes in climate were to result in a change to the
284 persistence and/or stability of the landfast ice in Porpoise Bay, it may result in detrimental
285 effects on glacier tongue stability. An important question, therefore, is: what process(es) cause
286 sea-ice break-up?

287 **5.2 What caused the January 2007 and March 2016 sea-ice break-ups?**

288 The majority of sea-ice in Porpoise Bay is multi-year sea-ice (Fraser et al., 2012), and it is
289 likely that various climatic processes operating over different timescales contributed to the
290 January 2007 sea-ice break-up event. Although there are no long-term observations of multi-
291 year sea-ice thickness in Porpoise Bay, observations and models of the annual cycle of multi-
292 year sea-ice in other regions of East Antarctica suggest that multi-year sea-ice thickens
293 seasonally and thins each year (Lei et al., 2010; Sugimoto et al., 2016; Yang et al., 2016).
294 Therefore, the relative strength, stability and thickness of multi-year sea ice at a given time
295 period is driven not only by synoptic conditions in the short term (days/weeks), but also by
296 climatic conditions in the preceding years.

297 In the austral summer (2005/06) which preceded the break-up event in January 2007, there was
298 a strong easterly airflow anomaly throughout December 2005 directly adjacent to Porpoise Bay
299 (Fig. 9a). This anomaly represents the weakening of the band of westerly winds which encircle
300 Antarctica, and is reflected in an exceptionally negative Southern Annular Mode (SAM) index
301 in December 2005 (Marshall, 2003). This contrasts with the long-term trend for a positive SAM
302 index (Marshall, 2007; Miles et al., 2013). A weaker band of westerly winds combined with
303 anomalously high SST in the Southern Pacific (Fig. 9a) would allow a greater advection of
304 warmer maritime air towards Porpoise Bay. Indeed, RACMO2.3 derived surface melt
305 estimates place December 2005 as the second highest mean melt month (1979-2015) on the
306 modelled output in Porpoise Bay (Fig. 10). To place this month into perspective, we note that it
307 would rank above the average melt values of all Decembers and Januarys since 2000 on the
308 remnants of Larsen B ice shelf. Comparing MODIS satellite imagery from before and after
309 December 2005 reveals the development of significant fracturing in the multi-year sea-ice (Fig
310 13a, b). These same fractures remain visible prior to the break-out event in January 2007 and,
311 when the multi-year sea-ice begins to break-up, it ruptures along these pre-existing weaknesses
312 (Fig. 13c). As such, this strongly suggests that the atmospheric circulation anomalies of

313 December 2005 played an important role in the January 2007 multi-year sea-ice break-up and
314 near-simultaneous calving event.

315 The break-up of landfast sea-ice has been linked to dynamic wind events and ocean swell
316 (Heil, 2006; Ushio, 2006; Fraser et al., 2012). Thus, it is possible that the wind anomalies in
317 December 2005 may have been important in initiating the fractures observed in the sea-ice in
318 Porpoise Bay, through changing the direction and/or intensity of oceanic swell. However, this
319 mechanism is thought to be at its most potent during anonymously low pack-ice concentrations
320 because pack-ice can act as a buffer to any oceanic swell (Langhorne et al., 2001; Heil, 2006;
321 Fraser, 2012). That said, we note that pack-ice concentrations offshore of Porpoise Bay were
322 around average during December 2005 (Fig. 7). This may suggest that there are other
323 mechanisms that were important in the weakening of the multi-year sea-ice in Porpoise Bay in
324 December 2005.

325 In the Arctic, sea-ice melt ponding along pre-existing weaknesses has been widely reported to
326 precede sea-ice break-up (Ehn et al., 2011; Petrich et al., 2012; Landy et al., 2014; Schroder et
327 al., 2014; Arntsen et al., 2015). Despite its importance in the Arctic, it has yet to be considered
328 as a possible factor in landfast sea-ice break-up in coastal Antarctica. As a consequence of the
329 high melt throughout December 2005, the growth of sea-ice surface ponding would be
330 expected, in addition to surface thinning of the sea-ice. High-resolution cloud free optical
331 satellite coverage of Porpoise Bay throughout December 2005 is limited, but ASTER imagery
332 in the vicinity of Frost Glacier on the 4th and 31st December 2005 shows surface melt features
333 and the development of fractures throughout the month (Fig. 13d,e), similar to those observed
334 elsewhere in East Antarctica (Kingslake et al., 2015; Langley et al., 2016). High-resolution
335 imagery from 16th January 2006 (via GoogleEarth) shows the development of melt ponds on
336 the sea-ice surface (Fig. 13f). Therefore, it is possible that surface melt had some impact on the
337 fracturing of landfast sea-ice in Porpoise Bay. This may have caused hydro-fracturing of pre-
338 existing depressions in the landfast ice or surface thinning may have made it more vulnerable
339 to fracturing through ocean swell or internal stresses. Additionally, the subsequent refreezing
340 of some melt ponds may temporally inhibit basal ice growth, potentially weakening the multi-
341 year sea-ice and predisposing it to future break-up (Flocco et al., 2015). It is important to note
342 that the atmospheric circulation anomalies which favoured the development of fractures in the
343 multi-year sea-ice in December 2005 were short-lived. By January 2006, atmospheric
344 conditions had returned close to average (Fig. 9b) and remained so until the austral winter,
345 where sea-ice break-up is less likely. This may explain the lag between the onset of sea-ice

346 fracturing in December 2005 and its eventual break-up in the following summer (January
347 2007).

348 Consistent with the notion that the multi-year sea-ice was already in a weakened state prior to
349 its break-up in 2007, is that the break-up occurred in January, several weeks before the likely
350 annual minimums in multi-year sea-ice thickness (Yang et al., 2016; Lei et al., 2010) and
351 landfast ice extent (Fraser et al., 2012). Additionally, atmospheric circulation anomalies
352 indicate little deviation from average conditions in the immediate months preceding break-up
353 (Fig. 9b, c), suggesting that atmospheric conditions were favourable for sea-ice stability.
354 Despite this, a synoptic event is still likely required to force the break-up in January 2007.
355 Daily sea-ice concentrations in Porpoise Bay in January 2007 January show a sharp decrease in
356 sea-ice concentrations after 12th January, representing the onset of sea-ice break-out (Fig 14).
357 This is preceded by a strong melt event recorded by the RACMO2.3 model, centred on January
358 11th, which may represent a low pressure system. Indeed, ERA-interim estimates of the wind
359 field suggest strong south-easterly winds in the vicinity of Porpoise Bay (Fig 11 a). Unlike in
360 December 2005, pack ice concentrations offshore of Porpoise Bay were anonymously low
361 (Fig. 7). Therefore, with less pack ice buttressing, it is possible that the melt event, high winds
362 and associated ocean swell may have initiated the break-up of the already weakened multi-year
363 sea-ice in Porpoise Bay.

364 In contrast to January 2007, we find no link between atmospheric circulation anomalies and
365 the March 2016 sea-ice break-up. In the preceding months to the March 2016 break-up, wind
366 and SST anomalies indicate conditions close to average conditions favouring sea-ice stability
367 (Fig. 9 d, e, f). This suggests another process was important in driving the March 2016 sea-
368 ice break-up. A key difference between the 2007 and 2016 event is that the largest glacier in
369 the bay, Holmes (West), only calved in the 2016 event. Analysis of its calving cycle (Fig. 12)
370 indicates that it calves at roughly the same position in each cycle and that its relative position
371 in early 2016 suggests that calving was ‘overdue’ (Fig. 12). This indicates that the calving
372 cycle of Holmes (West) Glacier is not necessarily been driven by atmospheric circulation
373 anomalies. Instead, we suggest that as Holmes (West) Glacier advances, it slowly pushes the
374 multi-year sea-ice attached to its terminus further towards the open ocean to the point where
375 the sea-ice attached to the glacier tongue becomes more unstable. This could be influenced by
376 local bathymetry and oceanic circulation, but no observations are available. However, once
377 the multi-year sea-ice reaches an unstable state, break-up is still likely to be forced by a
378 synoptic event. This is consistent with our observations, where ERA-interim derived wind

379 fields show the presence of a low pressure system close to Porpoise Bay on the estimated date
380 of sea-ice break-up in March 2016 (Fig. 11 b). Whilst we suggest that the March 2016 sea-ice
381 break-up and subsequent calving of Holmes (West) is currently part of a predictable cycle,
382 we note that this could be vulnerable to change if any future changes in climate alter the
383 persistence and/or strength of the multi-year sea-ice, which is usually attached to the glacier
384 terminus.

385 **6. Conclusion**

386 We identify two large near-simultaneous calving events in January 2007 and March 2016
387 which were driven by the break-up of the multi-year landfast sea-ice which usually occupies
388 the bay. This provides a previously unreported mechanism for the rapid disintegration of
389 floating glacier tongues in East Antarctica, adding to the growing body of research linking
390 glacier tongue stability to the mechanical coupling of landfast ice (e.g. Khazander et al.,
391 2009; Massom et al., 2010). Our results suggest that multi-year sea-ice break-ups in 2007 and
392 2016 in Porpoise Bay were driven by different mechanisms. We link the 2007 event to
393 atmospheric circulation anomalies in December 2005 weakening multi-year sea-ice through a
394 combination of surface melt and a change in wind direction, prior to its eventual break-up in
395 2007. This is in contrast to the March 2016 event, which we suggest is part of a longer-term
396 cycle based on the terminus position of Holmes (West) Glacier that was able to advance and
397 push sea-ice out of the bay. The link between sea-ice break-up and major calving of glacier
398 tongues is especially important because it suggests predictions of future warming (DeConto
399 and Pollard, 2016) suggests that multi-year landfast ice may become less persistent.
400 Therefore, the glacier tongues which depend on landfast ice for stability may become less
401 stable in the future. In a wider context, our results also highlight the complex nature of the
402 mechanisms which drive glacier calving position in Antarctica. Whilst regional trends in
403 terminus position can be driven by ocean-climate-sea-ice interaction (e.g. Miles et al., 2013;
404 2016), individual glaciers and individual calving events have the potential respond differently
405 to similar climatic forcing.

406

407 **Acknowledgements:** We thank the ESA for providing Envisat ASAR WSM data (Project ID:
408 16713) and Sentinel data. Landsat imagery was provided free of charge by the U.S. Geological
409 Survey Earth Resources Observation Science Centre. We thank M. van den Broeke for
410 providing data and assisting with RACMO. B.W.J.M was funded by a Durham University

411 Doctoral Scholarship program. S.S.R.J. was supported by Natural Environment Research
412 Council Fellowship NE/J018333/1. We would like to thank Allen Pope and Ted Scambos for
413 reviewing the manuscript, along with the editor, Rob Bingham, for providing constructive
414 comments which led to its improvement of this manuscript.

415

416 **References**

- 417 Aitken, A. R. A., Roberts, J. L., van Ommen, T. D., Young, D. A., Golledge, N. R.,
418 Greenbaum, J. S., Blankenship, D. D., and Siegert, M. J.: Repeated large-scale retreat and
419 advance of Totten Glacier indicated by inland bed erosion, *Nature*, 533, 385–+,
420 10.1038/nature17447, 2016.
- 421 Amundson, J. M., Fahnestock, M., Truffer, M., Brown, J., Luthi, M. P., and Motyka, R. J.: Ice
422 melange dynamics and implications for terminus stability, Jakobshavn Isbrae Greenland, *J*
423 *Geophys Res-Earth*, 115, Artn F01005 Doi 10.1029/2009jf001405, 2010.
- 424 Arntsen, A. E., Song, A. J., Perovich, D. K., and Richter-Menge, J. A.: Observations of the
425 summer breakup of an Arctic sea ice cover, *Geophys Res Lett*, 42, 8057-8063,
426 10.1002/2015GL065224, 2015.
- 427 Astrom, J. A., Vallot, D., Schafer, M., Welty, E. Z., O'Neel, S., Bartholomaeus, T. C., Liu, Y.,
428 Riikila, T. I., Zwinger, T., Timonen, J., and Moore, J. C.: Termini of calving glaciers as self-
429 organized critical systems, *Nat Geosci*, 7, 874-878, 10.1038/NGEO2290, 2014.
- 430 Banwell, A. F., MacAyeal, D. R., and Sergienko, O. V.: Breakup of the Larsen B Ice Shelf
431 triggered by chain reaction drainage of supraglacial lakes, *Geophys Res Lett*, 40, 5872-5876,
432 10.1002/2013GL057694, 2013.
- 433 Bassis, J. N., and Jacobs, S.: Diverse calving patterns linked to glacier geometry, *Nat Geosci*,
434 6, 833-836, 10.1038/NGEO1887, 2013.
- 435 Benn, D. I., Warren, C. R., and Mottram, R. H.: Calving processes and the dynamics of calving
436 glaciers, *Earth-Sci Rev*, 82, 143-179, 10.1016/j.earscirev.2007.02.002, 2007.
- 437 Cassotto, R., Fahnestock, M., Amundson, J. M., Truffer, M., and Joughin, I.: Seasonal and
438 interannual variations in ice melange and its impact on terminus stability, Jakobshavn Isbrae,
439 Greenland, *J Glaciol*, 61, 76-88, 10.3189/2015JoG13J235, 2015.
- 440 Chapuis, A., and Tetzlaff, T.: The variability of tidewater-glacier calving: origin of event-size
441 and interval distributions, *J Glaciol*, 60, 622-634, 10.3189/2014JoG13J215, 2014.
- 442 Comiso, J. C.: Bootstrap Sea Ice Concentrations from Nimbus-7 SMMR and DMSP SSM/I-
443 SSMIS. Version 2, Boulder, Colorado USA: NASA National Snow and Ice Data Center
444 Distributed Active Archive Center., 2014.

445 Cook, A. J., Fox, A. J., Vaughan, D. G., and Ferrigno, J. G.: Retreating Glacier Fronts on the
446 Antarctic Peninsula over the Past Half-Century, *Science*, 308, 541-544,
447 10.1126/science.1104235, 2005.

448 Cook, C. P., Hill, D. J., van de Flierdt, T., Williams, T., Hemming, S. R., Dolan, A. M., Pierce,
449 E. L., Escutia, C., Harwood, D., Cortese, G., and Gonzales, J. J.: Sea surface temperature
450 control on the distribution of far-traveled Southern Ocean ice-rafted detritus during the
451 Pliocene, *Paleoceanography*, 29, 533-548, Doi 10.1002/2014pa002625, 2014.

452 De Angelis, H., and Skvarca, P.: Glacier surge after ice shelf collapse, *Science*, 299, 1560-
453 1562, DOI 10.1126/science.1077987, 2003.

454 DeConto, R. M., and Pollard, D.: Contribution of Antarctica to past and future sea-level rise,
455 *Nature*, 531, 591-+, 10.1038/nature17145, 2016.

456 Depoorter, M. A., Bamber, J. L., Griggs, J. A., Lenaerts, J. T. M., Ligtenberg, S. R. M., van
457 den Broeke, M. R., and Moholdt, G.: Calving fluxes and basal melt rates of Antarctic ice
458 shelves, *Nature*, 502, 89-+, Doi 10.1038/Nature12567, 2013.

459 Ehn, J. K., Mundy, C. J., Barber, D. G., Hop, H., Rossnagel, A., and Stewart, J.: Impact of
460 horizontal spreading on light propagation in melt pond covered seasonal sea ice in the
461 Canadian Arctic, *J Geophys Res-Oceans*, 116, Artn C00g02 10.1029/2010jc006908, 2011.

462 Flocco, D., Feltham, D. L., Bailey, E., and Schroeder, D.: The refreezing of melt ponds on
463 Arctic sea ice, *J Geophys Res-Oceans*, 120, 647-659, 10.1002/2014JC010140, 2015.

464 Fraser, A. D., Massom, R. A., Michael, K. J., Galton-Fenzi, B. K., and Lieser, J. L.: East
465 Antarctic Landfast Sea Ice Distribution and Variability, 2000-08, *J Climate*, 25, 1137-1156,
466 10.1175/Jcli-D-10-05032.1, 2012.

467 Frezzotti, M., and Polizzi, M.: 50 years of ice-front changes between the Adelie and Banzare
468 Coasts, East Antarctica, *Ann Glaciol*, 34, 235-240, 10.3189/172756402781817897, 2002.

469 Fürst, J.J., Durand, G., Gillet-Chaulet, F., Tavard, L., Rankl, M., Braun, M., and Gagliardini,
470 O.: The safety band of Antarctic ice shelves. *Nature. Clim. Chan.*, 6, 479-481, 2016.

471 Greenbaum, J. S., Blankenship, D. D., Young, D. A., Richter, T. G., Roberts, J. L., Aitken, A.
472 R. A., Legresy, B., Schroeder, D. M., Warner, R. C., van Ommen, T. D., and Siegert, M. J.:
473 Ocean access to a cavity beneath Totten Glacier in East Antarctica, *Nat Geosci*, 8, 294-298,
474 10.1038/NGEO2388, 2015.

475 Heil, P.: Atmospheric conditions and fast ice at Davis, East Antarctica: A case study, *J*
476 *Geophys Res-Oceans*, 111, Artn C05009 10.1029/2005jc002904, 2006.

477 Khazendar, A., Rignot, E., and Larour, E.: Roles of marine ice, rheology, and fracture in the
478 flow and stability of the Brunt/Stancomb-Wills Ice Shelf, *J Geophys Res-Earth*, 114, Artn
479 F04007 10.1029/2008jf001124, 2009.

480 Kim, K., Jezek, K. C., and Liu, H.: Orthorectified image mosaic of Antarctica from 1963
481 Argon satellite photography: image processing and glaciological applications, *Int J Remote*
482 *Sens*, 28, 5357-5373, 2007.

483 King, M. A., Bingham, R. J., Moore, P., Whitehouse, P. L., Bentley, M. J., and Milne, G. A.:
484 Lower satellite-gravimetry estimates of Antarctic sea-level contribution, *Nature*, 491, 586-+,
485 Doi 10.1038/Nature11621, 2012.

486 Kingslake, J., Ng, F., and Sole, A.: Modelling channelized surface drainage of supraglacial
487 lakes. *J. Glaciol.*, 61 (225), 185-199, 2015.

488 Landy, J., Ehn, J., Shields, M., and Barber, D.: Surface and melt pond evolution on landfast
489 first-year sea ice in the Canadian Arctic Archipelago, *J Geophys Res-Oceans*, 119, 3054-3075,
490 10.1002/2013JC009617, 2014.

491 Langhorne, P. J., Squire, V. A., Fox, C., and Haskell, T. G.: Lifetime estimation for a land-fast
492 ice sheet subjected to ocean swell, *Annals of Glaciology*, Vol 33, 33, 333-338, Doi
493 10.3189/172756401781818419, 2001.

494 Langlais, C. E., Rintoul, S. R., and Zika, J. D.: Sensitivity of Antarctic Circumpolar Current
495 Transport and Eddy Activity to Wind Patterns in the Southern Ocean, *J Phys Oceanogr*, 45,
496 1051-1067, 10.1175/Jpo-D-14-0053.1, 2015.

497 Langley, E.S., Leeson, A.A., Stokes, C.R., and Jamieson, S.S.R.: Seasonal evolution of
498 supraglacial lakes on an East Antarctic outlet glacier. *Geophys. Res. Lett.*, 43,
499 doi:10.1002/2016GL069511,

500 Lei, R. B., Li, Z. J., Cheng, B., Zhang, Z. H., and Heil, P.: Annual cycle of landfast sea ice in
501 Prydz Bay, east Antarctica, *J Geophys Res-Oceans*, 115, Artn C02006 10.1029/2008jc005223,
502 2010.

503 Liu, H. X., and Jezek, K. C.: A complete high-resolution coastline of antarctica extracted from
504 orthorectified Radarsat SAR imagery, *Photogramm Eng Rem S*, 70, 605-616, 2004.

505 Mahoney, A., Eicken, H., Gaylord, A. G., and Shapiro, L.: Alaska landfast sea ice: Links with
506 bathymetry and atmospheric circulation, *J Geophys Res-Oceans*, 112, Artn C02001
507 10.1029/2006jc003559, 2007.

508 Marshall, G. J.: Trends in the southern annular mode from observations and reanalyses, *J*
509 *Climate*, 16, 4134-4143, Doi 10.1175/1520-0442(2003)016<4134:Titsam>2.0.Co;2, 2003.

510 Marshall, G. J.: Half-century seasonal relationships between the Southern Annular Mode and
511 Antarctic temperatures, *Int J Climatol*, 27, 373-383, 10.1002/joc.1407, 2007.

512 Massom, R. A., Giles, A. B., Warner, R. C., Fricker, H. A., Legresy, B., Hyland, G.,
513 Lescarontier, L., and Young, N.: External influences on the Mertz Glacier Tongue (East
514 Antarctica) in the decade leading up to its calving in 2010, *J Geophys Res-Earth*, 120, 490-506,
515 10.1002/2014JF003223, 2015.

516 McMillan, M., Shepherd, A., Sundal, A., Briggs, K., Muir, A., Ridout, A., Hogg, A., and
517 Wingham, D.: Increased ice losses from Antarctica detected by CryoSat-2, *Geophys Res Lett*,
518 41, 3899-3905, Doi 10.1002/2014gl060111, 2014.

519 Miles, B. W. J., Stokes, C. R., Vieli, A., and Cox, N. J.: Rapid, climate-driven changes in
520 outlet glaciers on the Pacific coast of East Antarctica, *Nature*, 500, 563-+, Doi
521 10.1038/Nature12382, 2013.

522 Miles, B. W. J., Stokes, C. R., and Jamieson, S. S. R.: Pan-ice-sheet glacier terminus change in
523 East Antarctica reveals sensitivity of Wilkes Land to sea-ice changes, *Science Advances*, 2,
524 10.1126/sciadv.1501350, 2016.

525 Moon, T., and Joughin, I.: Changes in ice front position on Greenland's outlet glaciers from
526 1992 to 2007, *J Geophys Res-Earth*, 113, Artn F02022 Doi 10.1029/2007jf000927, 2008.

527 Parkinson, C. L., J. C. Comiso, and H. J. Zwally. 1999, updated 2004. *Nimbus-5 ESMR Polar*
528 *Gridded Sea Ice Concentrations*. Edited by W. Meier and J. Stroeve. Boulder, Colorado USA:
529 National Snow and Ice Data Center. Digital media.

530 Petrich, C., Eicken, H., Polashenski, C. M., Sturm, M., Harbeck, J. P., Perovich, D. K., and
531 Finnegan, D. C.: Snow dunes: A controlling factor of melt pond distribution on Arctic sea ice,
532 *J Geophys Res-Oceans*, 117, Artn C0902910.1029/2012jc008192, 2012.

533 Pritchard, H. D., Arthern, R. J., Vaughan, D. G., and Edwards, L. A.: Extensive dynamic
534 thinning on the margins of the Greenland and Antarctic ice sheets, *Nature*, 461, 971-975,
535 10.1038/nature08471, 2009.

536 Rignot, E., Casassa, G., Gogineni, P., Krabill, W., Rivera, A., and Thomas, R.: Accelerated ice
537 discharge from the Antarctic Peninsula following the collapse of Larsen B ice shelf, *Geophys*
538 *Res Lett*, 31, Artn L1840110.1029/2004gl020697, 2004.

539 Rignot, E., Mouginot, J., and Scheuchl, B.: Ice Flow of the Antarctic Ice Sheet, *Science*, 333,
540 1427-1430, 10.1126/science.1208336, 2011.

541 Rignot, E., Jacobs, S., Mouginot, J., and Scheuchl, B.: Ice-Shelf Melting Around Antarctica,
542 *Science*, 341, 266-270, DOI 10.1126/science.1235798, 2013.

543 Rott, H., Skvarca, P., and Nagler, T.: Rapid collapse of northern Larsen Ice Shelf, *Antarctica*,
544 *Science*, 271, 788-792, DOI 10.1126/science.271.5250.788, 1996.

545 Rott, H., Rack, W., Skvarca, P., and De Angelis, H.: Northern Larsen Ice Shelf, Antarctica:
546 further retreat after collapse, *Annals of Glaciology*, Vol 34, 2002, 34, 277-282, Doi
547 10.3189/172756402781817716, 2002.

548 Sasgen, I., Konrad, H., Ivins, E. R., Van den Broeke, M. R., Bamber, J. L., Martinec, Z., and
549 Klemann, V.: Antarctic ice-mass balance 2003 to 2012: regional reanalysis of GRACE satellite
550 gravimetry measurements with improved estimate of glacial-isostatic adjustment based on GPS
551 uplift rates, *Cryosphere*, 7, 1499-1512, DOI 10.5194/tc-7-1499-2013, 2013.

552 Scambos, T., Hulbe, C., and Fahnestock, M.: Climate-induced ice shelf disintegration in the
553 Antarctic Peninsula, *Antarct Res Ser*, 79, 79-92, 2003.

554 Scambos, T., Fricker, H. A., Liu, C. C., Bohlander, J., Fastook, J., Sargent, A., Massom, R.,
555 and Wu, A. M.: Ice shelf disintegration by plate bending and hydro-fracture: Satellite
556 observations and model results of the 2008 Wilkins ice shelf break-ups, *Earth Planet Sc Lett*,
557 280, 51-60, 10.1016/j.epsl.2008.12.027, 2009.

558 Schroder, D., Feltham, D. L., Flocco, D., and Tsamados, M.: September Arctic sea-ice
559 minimum predicted by spring melt-pond fraction, *Nat Clim Change*, 4, 353-357,
560 10.1038/Nclimate2203, 2014.

561 Spreen, G., Kaleschke, L., and Heygster, G.: Sea ice remote sensing using AMSR-E 89-GHz
562 channels, *J Geophys Res-Oceans*, 113, Artn C02s0310.1029/2005jc003384, 2008.

563 Sugimoto, F., Tamura, T., Shimoda, H., Uto, S., Simizu, D., Tateyama, K., Hoshino, S., Ozeki,
564 T., Fukamachi, Y., Ushio, S., and Ohshima, K. I.: Interannual variability in sea-ice thickness in
565 the pack-ice zone off Lutzow-Holm Bay, East Antarctica, *Polar Sci*, 10, 43-51,
566 10.1016/j.polar.2015.10.003, 2016.

567 Todd, J., and Christoffersen, P.: Are seasonal calving dynamics forced by buttressing from ice
568 melange or undercutting by melting? Outcomes from full-Stokes simulations of Store Glacier,
569 West Greenland, *Cryosphere*, 8, 2353-2365, 10.5194/tc-8-2353-2014, 2014.

570 Ushio, S.: Factors affecting fast-ice break-up frequency in Lutzow-Holm bay, Antarctica,
571 *Annals of Glaciology*, Vol 44, 2006, 44, 177-182, Doi 10.3189/172756406781811835, 2006.

572 van der Veen, C. J.: Calving glaciers, *Prog Phys Geog*, 26, 96-122,
573 10.1191/0309133302pp327ra, 2002.

574 van Wessem, J. M., Reijmer, C. H., Morlighem, M., Mougnot, J., Rignot, E., Medley, B.,
575 Joughin, I., Wouters, B., Depoorter, M. A., Bamber, J. L., Lenaerts, J. T. M., van de Berg, W.
576 J., van den Broeke, M. R., and van Meijgaard, E.: Improved representation of East Antarctic
577 surface mass balance in a regional atmospheric climate model, *J Glaciol*, 60, 761-770,
578 10.3189/2014JoG14J051, 2014.

579 Wang, X., Holland, D. M., Cheng, X., and Gong, P.: Grounding and Calving Cycle of Mertz
580 Ice Tongue Revealed by Shallow Mertz Bank, *The Cryosphere Discuss.*, 2016, 1-37,
581 10.5194/tc-2016-3, 2016.

582 Wuite, J., Rott, H., Hetzenecker, M., Floricioiu, D., De Rydt, J., Gudmundsson, G. H., Nagler,
583 T., and Kern, M.: Evolution of surface velocities and ice discharge of Larsen B outlet glaciers
584 from 1995 to 2013, *Cryosphere*, 9, 957-969, 10.5194/tc-9-957-2015, 2015.

585 Yang, Y., Li, Z. J., Leppazranta, M., Cheng, B., Shi, L. Q., and Lei, R. B.: Modelling the
586 thickness of landfast sea ice in Prydz Bay, East Antarctica, *Antarct Sci*, 28, 59-70,
587 10.1017/S0954102015000449, 2016.

588 Young, D. A., Wright, A. P., Roberts, J. L., Warner, R. C., Young, N. W., Greenbaum, J. S.,
589 Schroeder, D. M., Holt, J. W., Sugden, D. E., Blankenship, D. D., van Ommen, T. D., and
590 Siegert, M. J.: A dynamic early East Antarctic Ice Sheet suggested by ice-covered fjord
591 landscapes, *Nature*, 474, 72-75, 10.1038/nature10114, 2011.

592

593

594

595

596

597

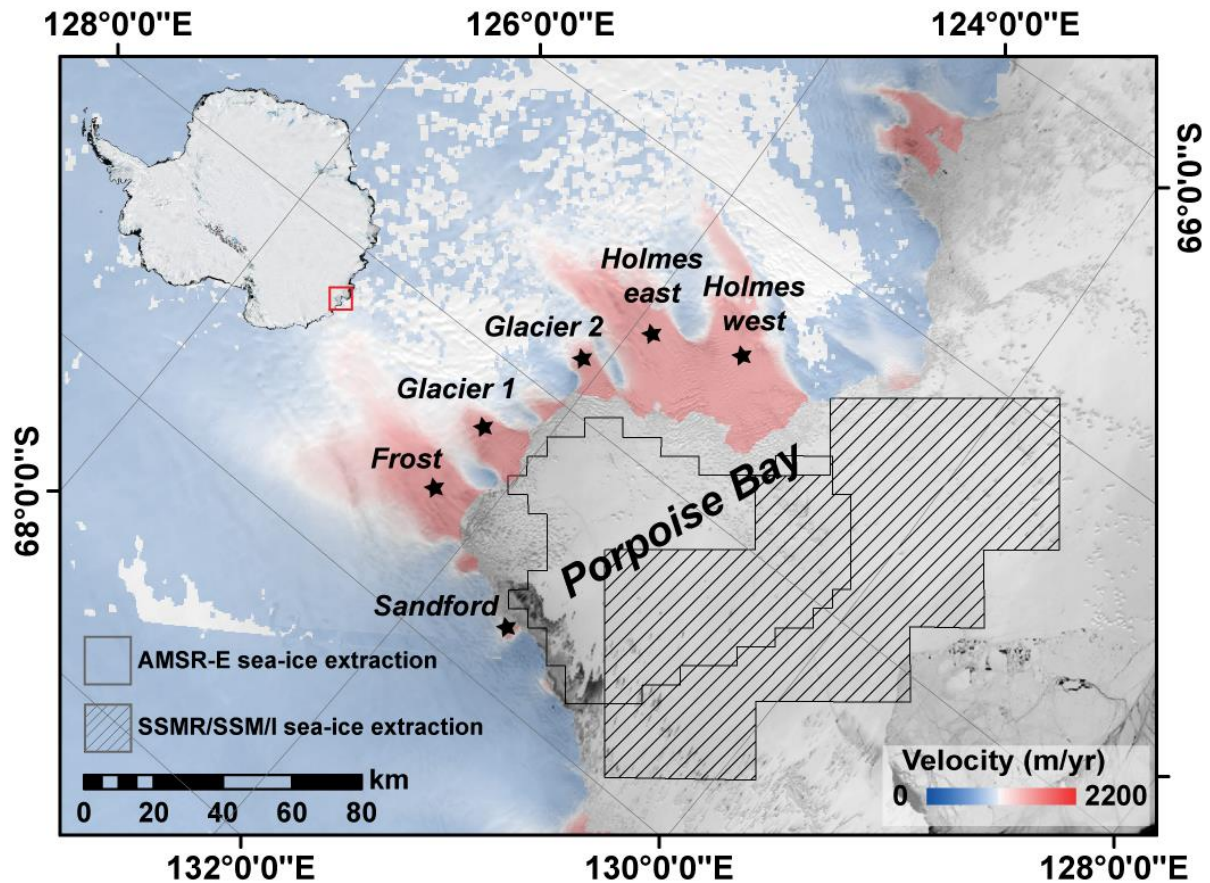
598

599 **Table 1: Satellite imagery used in the study**

Satellite	Date of Imagery
ARGON	October 1963 (Kim et al., 2007)
Envisat ASAR WSM	August 2002, November 2002 to March 2012 (monthly)
Landsat	January 1973; February 1991
MODIS	January 2001; December/January 2005/6; March 2016
RADARSAT	September 1997 (Liu and Jezek, 2004)
Sentinel-1	February-July, 2016

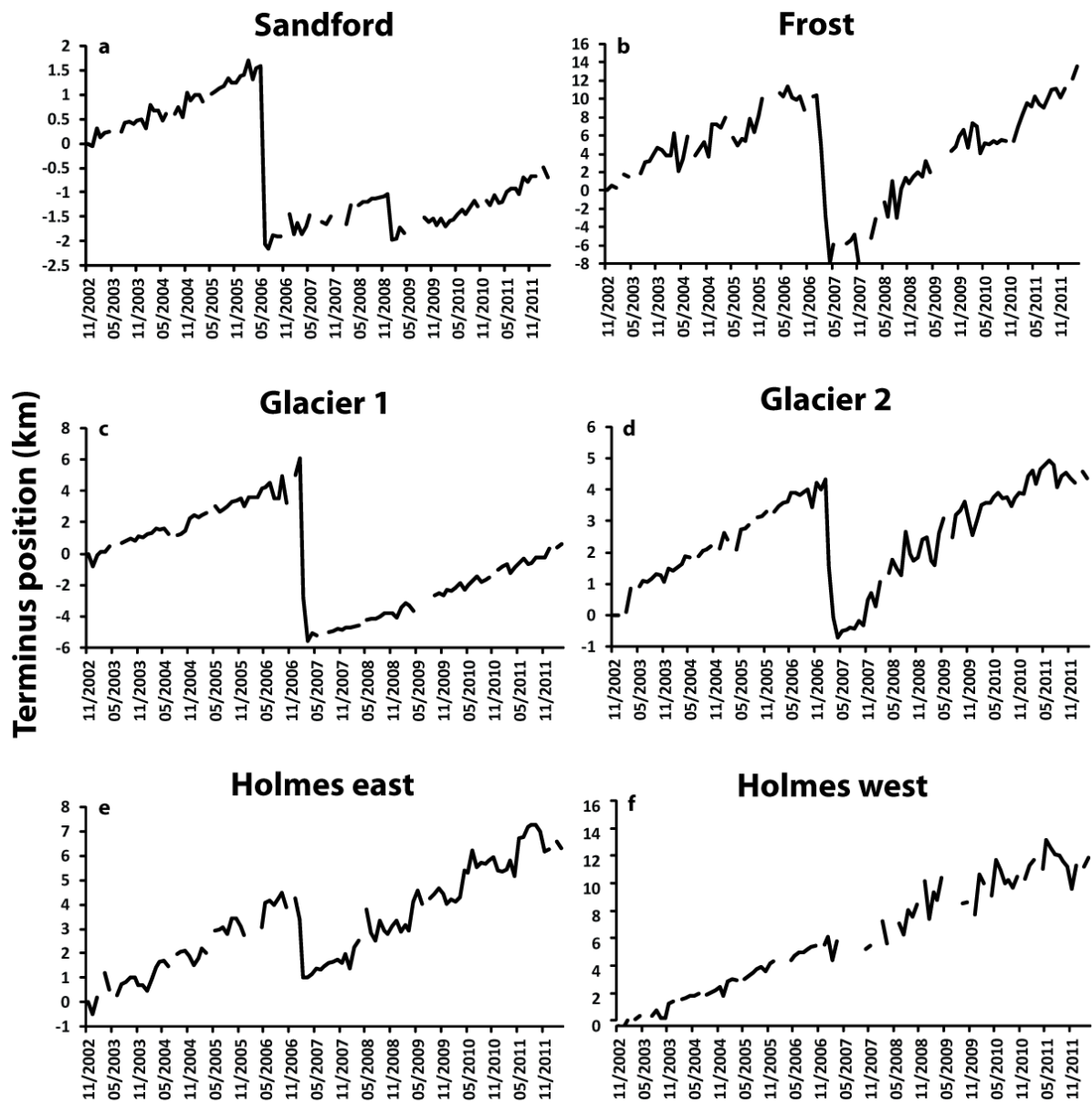
600

601



602

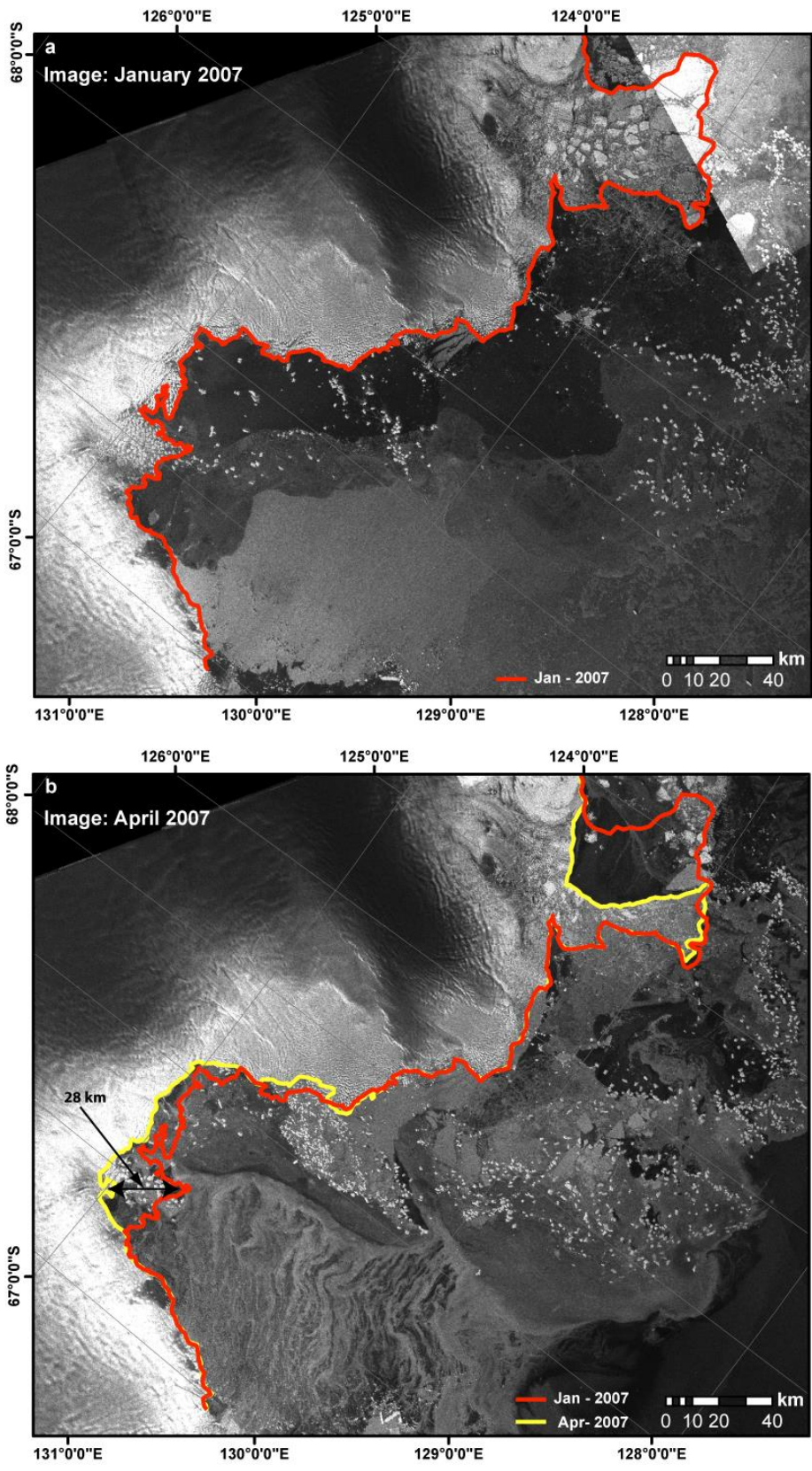
603 **Figure 1:** MODIS image of Porpoise Bay, with glacier velocities overlain (Rignot et al.,
 604 2011). The hatched polygon represents the region where long-term 25 km resolution
 605 SMMR/SSM/I sea-ice concentrations were extracted. The non-hatched polygon represents
 606 the region where the higher resolution (6.25 km) AMSR-E sea-ice concentrations were
 607 extracted.



608

609 **Figure 2:** Terminus position change of six glaciers in porpoise Bay between November 2002
 610 and March 2012. Note the major calving event in January 2007 for 5 of the glaciers.

611 Terminus position measurements are subject to +/- 500 m. Note the different scales on y-axis.



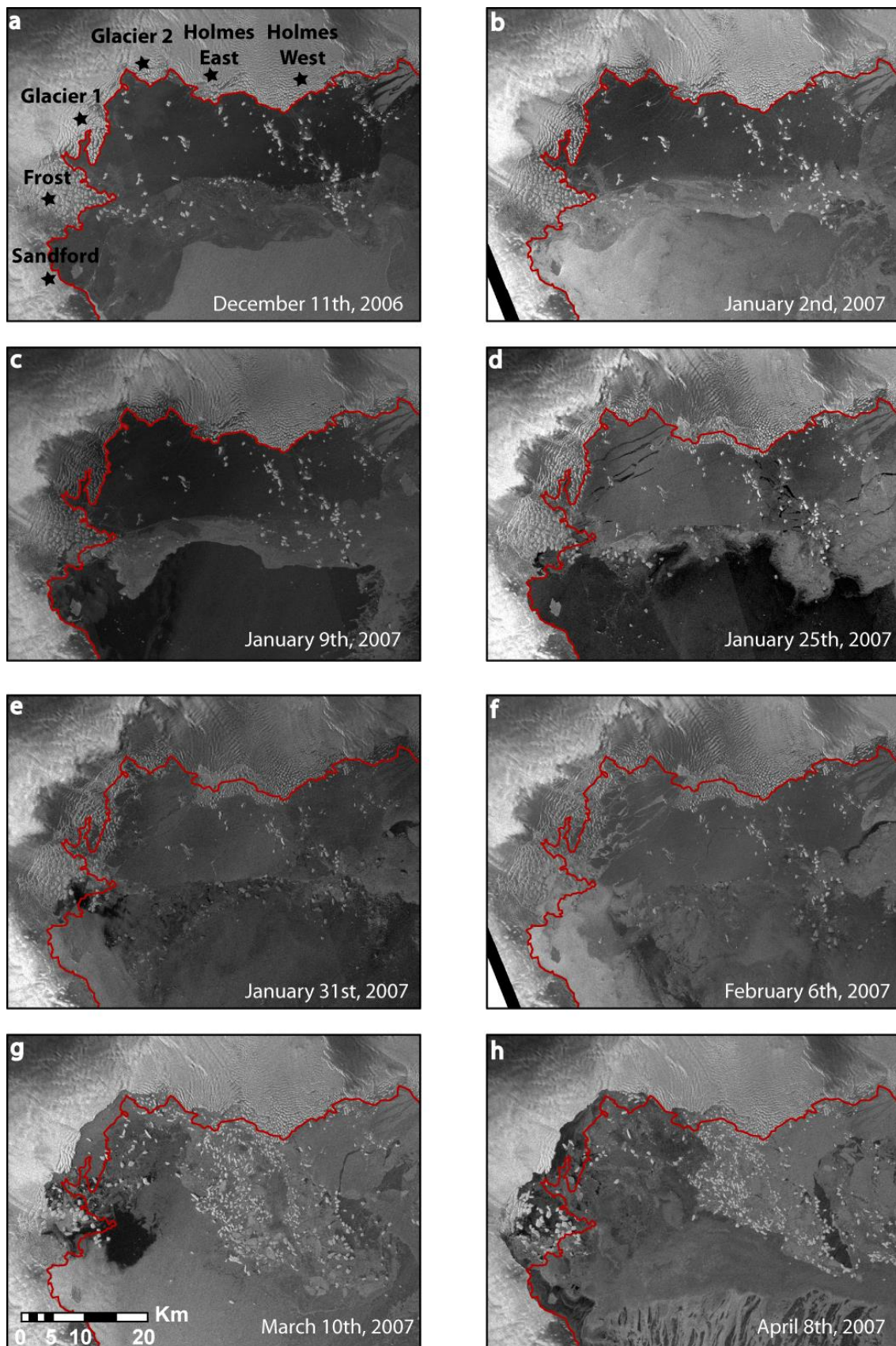
612

613

614

615

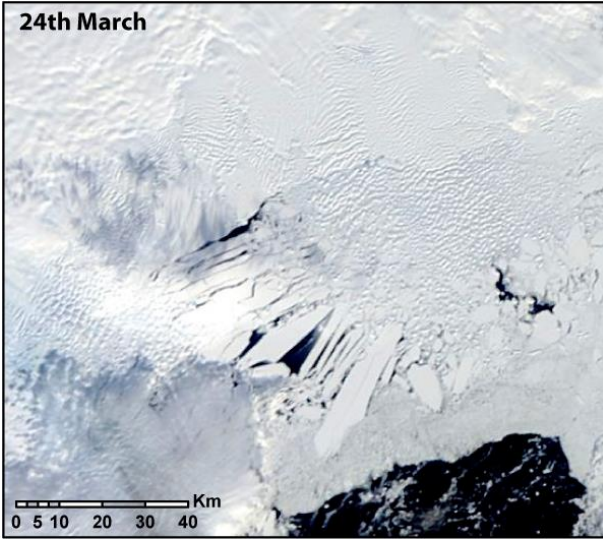
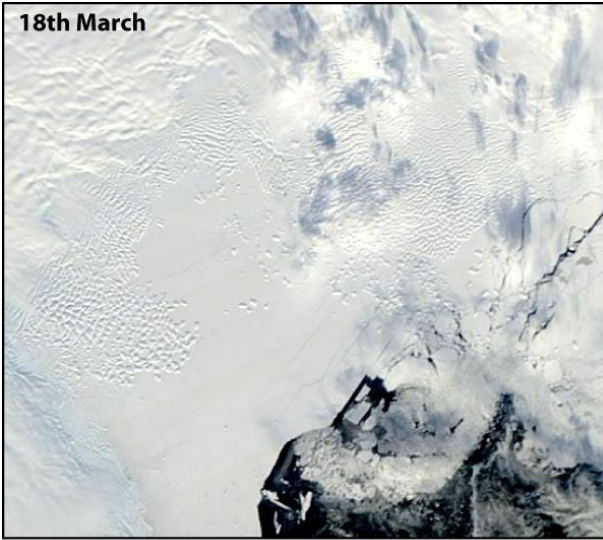
Figure 3: Envisat ASAR WSM imagery in January 2007 **a)** and April 2007 **b)**, which are immediately prior to and after a near-simultaneous calving event in Porpoise Bay. Red line shows terminus positions in January 2007 and yellow line shows the positions in April 2007.



616

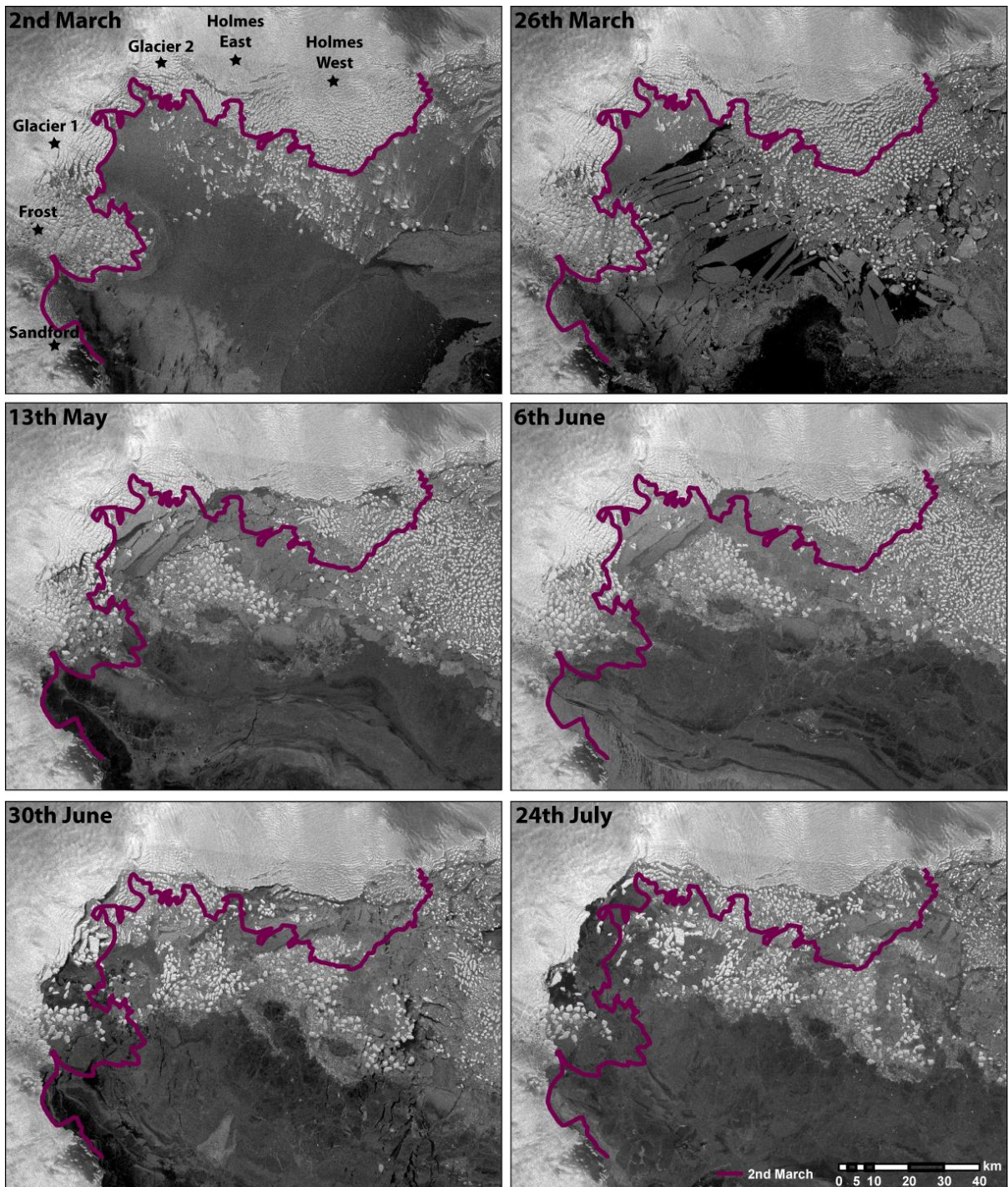
617 **Figure 4:** Envisat ASAR WSM imagery showing the evolution of the 2007 calving event.

618 Red line shows the terminus positions from December 11th 2006 on all panels.



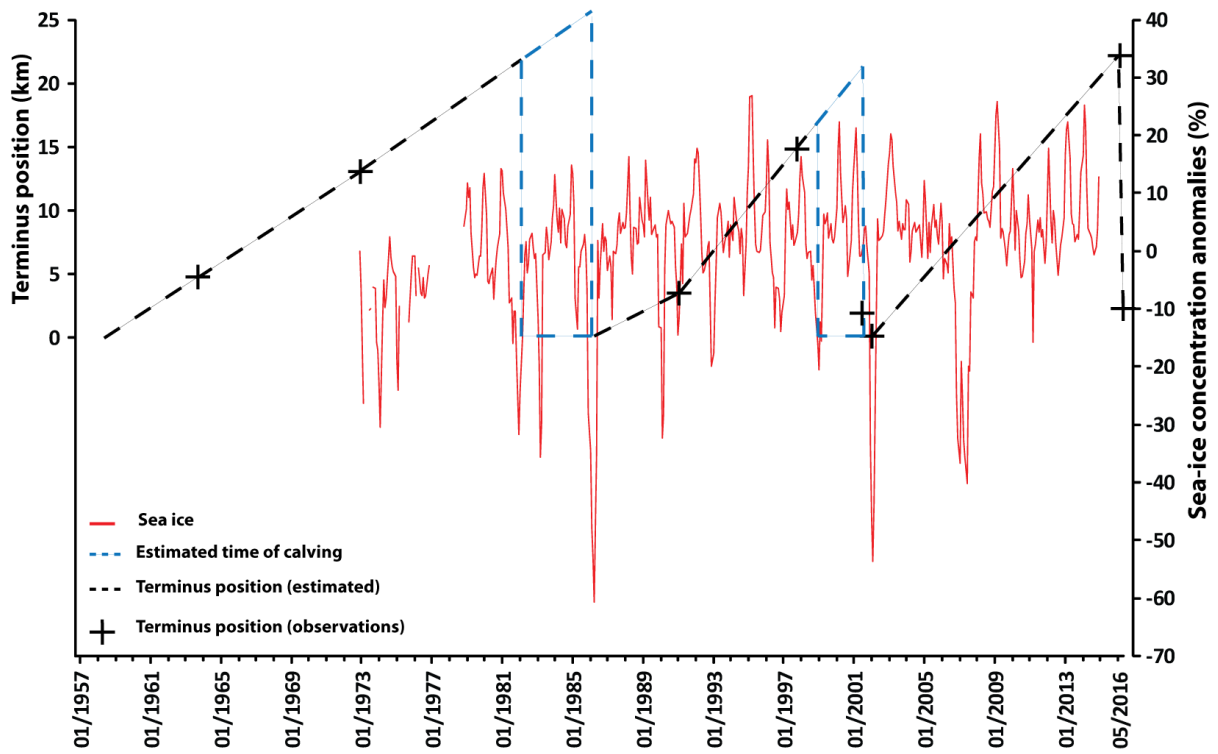
619

620 **Figure 5:** MODIS imagery showing the initial stages of disintegration of Holmes (West)
621 Glacier in March 2016. On March 19th a large section of sea-ice breaks away from the
622 terminus (circled), initiating the rapid disintegration process. By the 24th March an 800 km²
623 section of Holmes (west) glacier tongue had disintegrated.



625

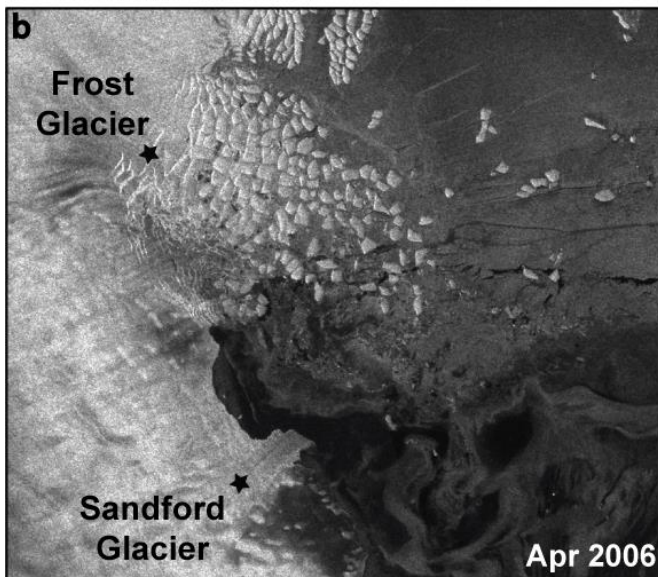
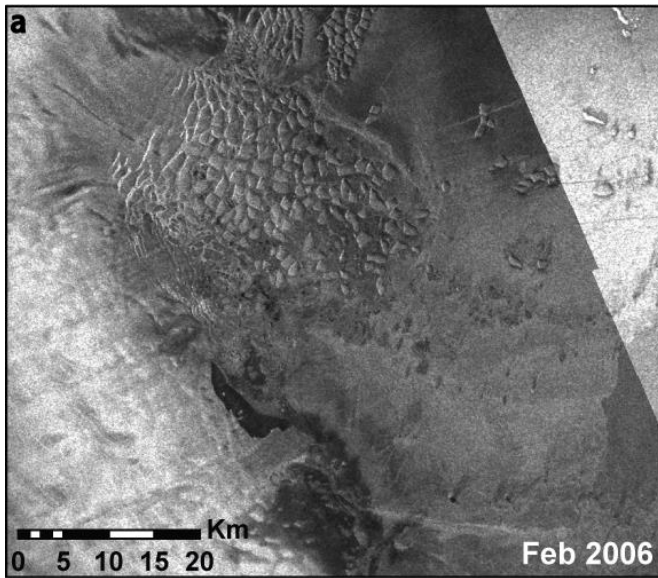
626 **Figure 6:** Sentinel-1 imagery showing the evolution of the 2016 calving event. Purple line
 627 shows the terminus position from 2nd March on all panels.



628

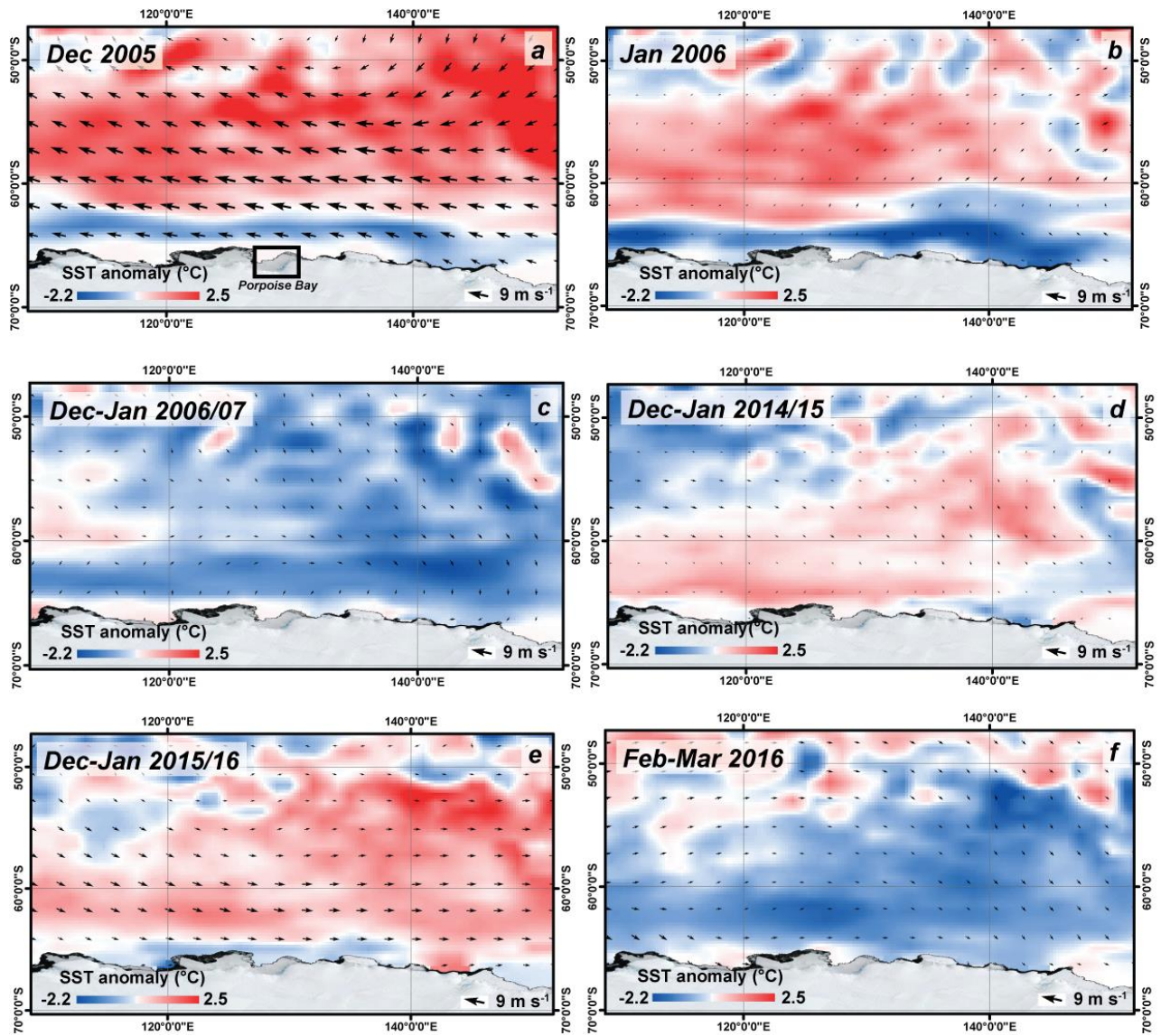
629 **Fig 7:** Mean monthly sea-ice concentration anomalies from November 2002 to June 2016.
 630 The red line indicates sea-ice concentration anomalies in Porpoise Bay and the blue line
 631 indicates pack ice concentration anomalies.

632



633

634 **Figure 8:** Time series of Frost and Sanford Glaciers calving showing that sea-ice clears prior
635 to calving and dispersal of icebergs.



636

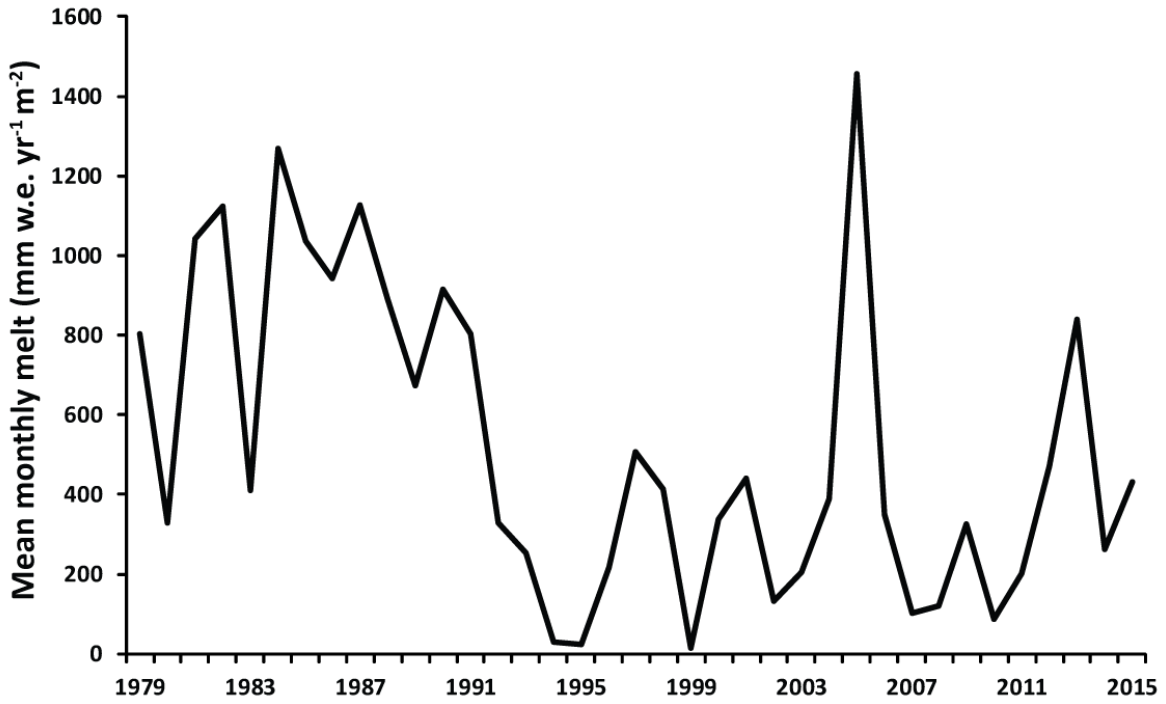
637

638

639

640

Figure 9: Mean monthly ERA-interim derived wind field and sea surface temperature anomalies in the months preceding the 2007 and 2016 sea-ice break-ups. **a)** December 2005 **b)** January 2006 **c)** Mean December and January 2006/07 **d)** Mean December and January 2014/15 **e)** Mean December and January 2015/16 **f)** Mean February and March 2016.



641

642 **Figure 10:** Mean RACMO2.3 derived December melt 1979-2015 in Porpoise Bay.

643

644

645

646

647

648

649

650

651

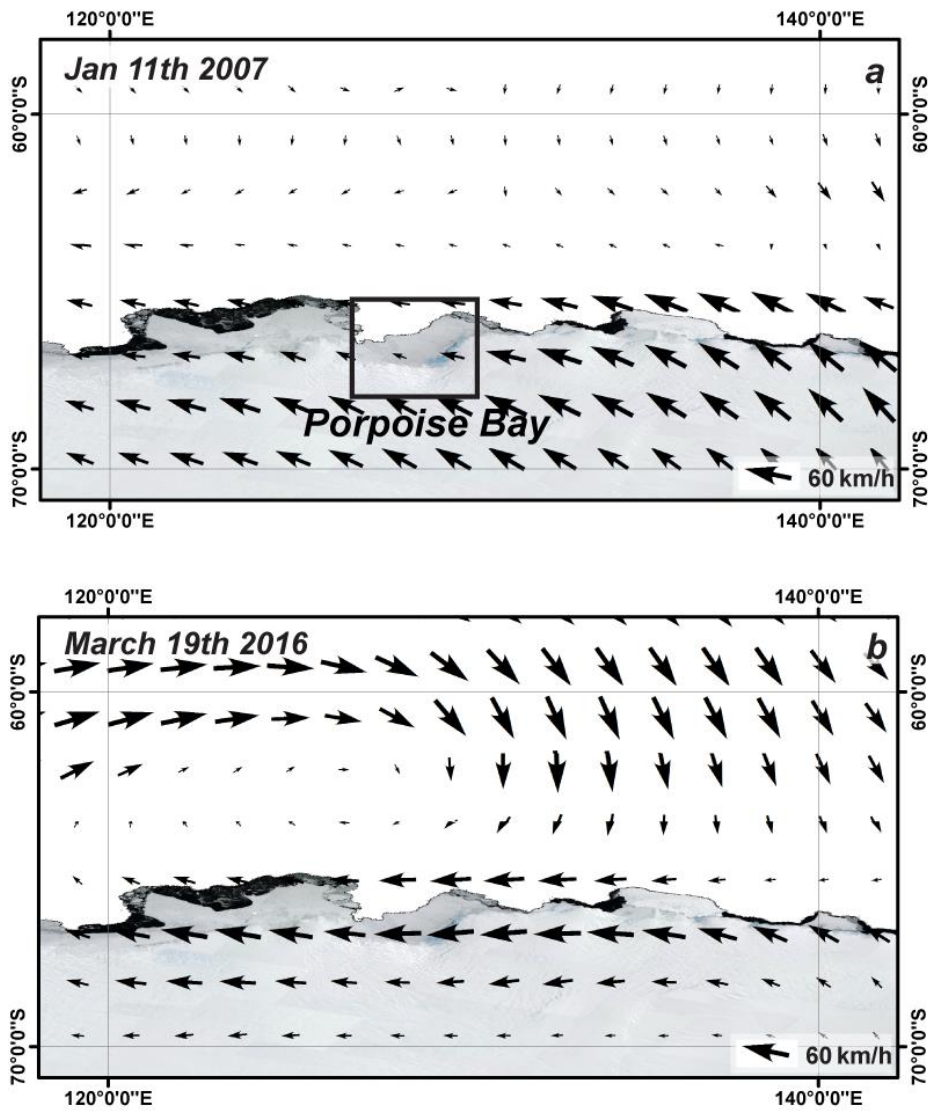
652

653

654

655

656



657

658 **Figure 11:** ERA-interim derived wind fields for the estimated dates of sea-ice break-up. **a)**
 659 January 11th 2007 and **b)** March 19th 2016.

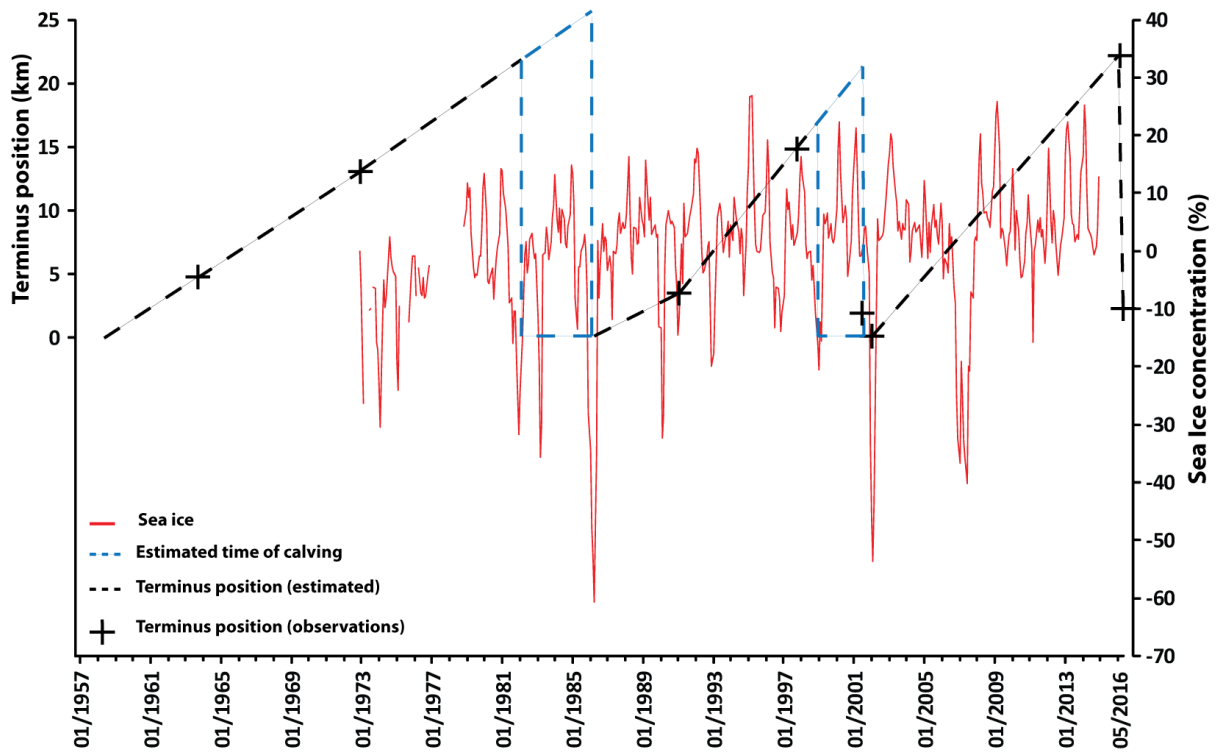
660

661

662

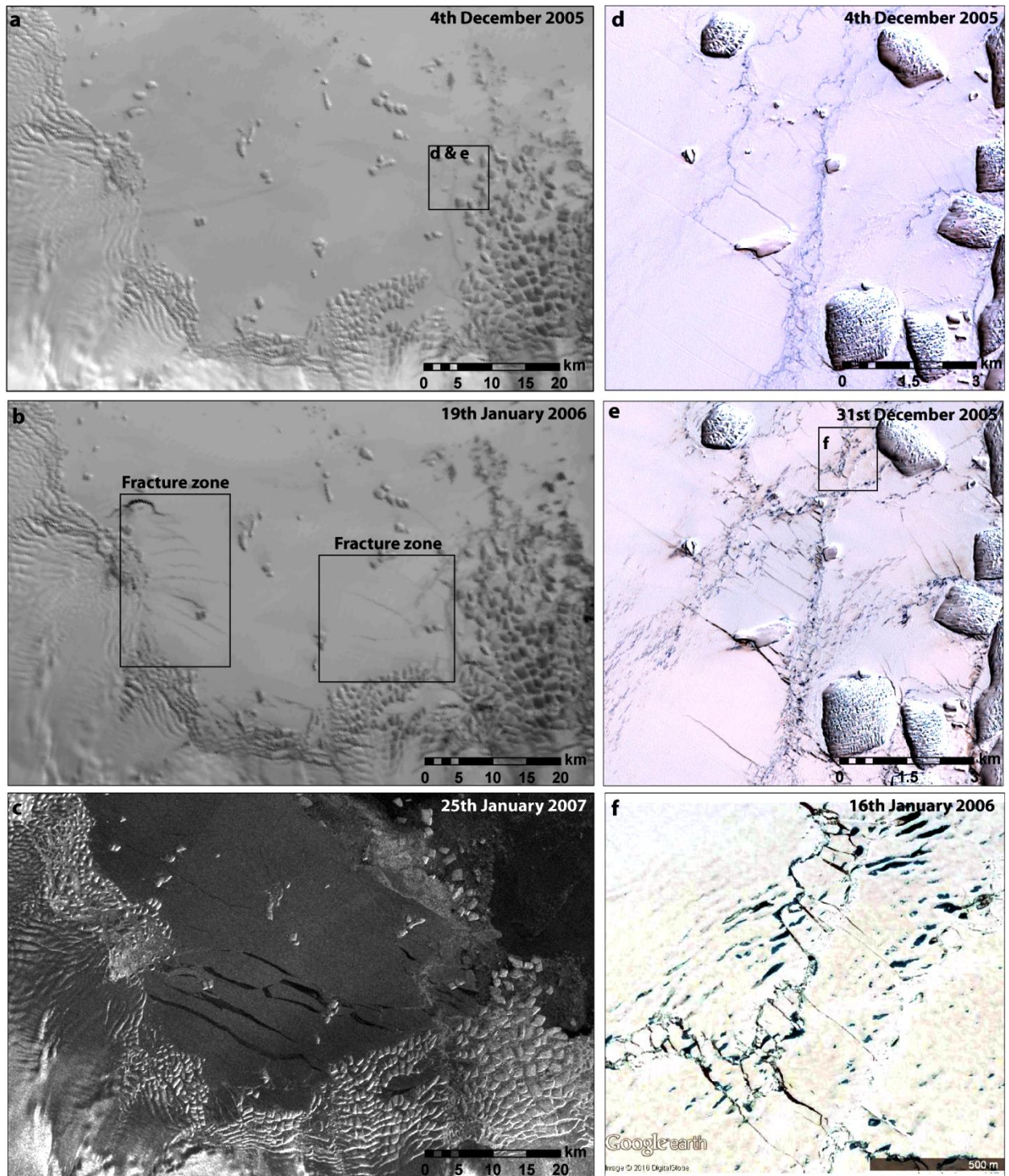
663

664



665
 666
 667
 668
 669
 670

Figure 12: Reconstruction of the calving cycle of Holmes (West) Glacier. All observations are represented by black crosses. The estimated terminus position is then extrapolated linearly between each observation. In periods without observations the date of calving is estimated by negative sea-ice concentration anomalies.



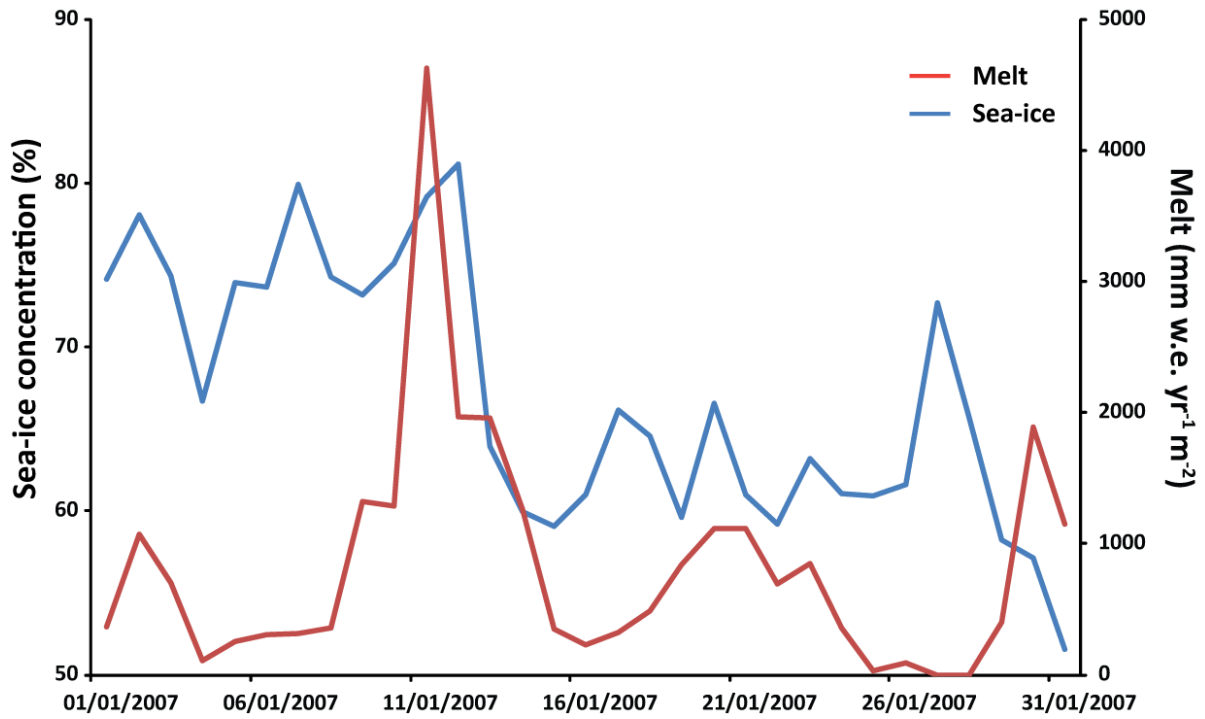
672

673 **Figure 13: a and b)** MODIS imagery showing the development of fractures in the landfast
 674 sea-ice between 4th December 2005 and 19th January 2006
 675 (<http://dx.doi.org/10.7265/N5NC5Z4N>.) **c)** The landfast sea-ice ruptures along some of the
 676 same fractures which formed in December/January 2005/06, eventually leading to complete
 677 break-up in January 2007. **d and e)** ASTER imagery showing surface melt features and the
 678 development of smaller fracture between 4th and 31st December 2005. **f)** High resolution

679 optical satellite imagery from 16th January 2006 showing sea-ice fracturing and surface melt
680 ponding. This image was obtained from Google Earth.

681

682



683

684 **Figure 14:** Daily sea-ice concentrations and RACMO derived melt during January 2007 in
685 Porpoise Bay. Sea-ice concentrations start to decrease after the melt peak on January 11th.

686

687

688

689

690

691

692

693